Available online at www.sciencedirect.com
SCIENCE DIRECT®
Biochemical Pharmacology 68 (2004) 1279–1288
Biochemical Pharmacology
www.elsevier.com/locate/biochempharm

The novel histone deacetylase inhibitor BL1521 inhibits proliferation and induces apoptosis in neuroblastoma cells

Annemieke J.M. de Ruijter, Stephan Kemp, Gertjan Kramer, Rutger J. Meinsma, Judith O. Kaufmann, Huib N. Caron, André B.P. van Kuilenburg*

Laboratory Genetic Metabolic Diseases, Department of Paediatrics/Emma Children's Hospital and Clinical Chemistry, Academic Medical Centre, University of Amsterdam, P.O. Box 22700, 1100 DE Amsterdam, The Netherlands

Received 9 January 2004; accepted 4 May 2004

Abstract

Neuroblastoma is a childhood cancer arising from the sympathetic nervous system. Disseminated neuroblastoma has a poor prognosis despite intensive multimodality treatment. Histone deacetylases (HDACs) were recently discovered as a potential target for pharmacological gene therapy in cancer. HDACs have an important function in regulating DNA packaging in chromatin, thereby affecting the transcription of genes.

In this paper, we tested the efficacy of a newly developed histone deacetylase inhibitor, BL1521, on neuroblastoma in vitro by investigating the changes in: acetylation of histone H3, in situ HDAC activity, $p21^{WAF1/CIP1}$ and *MYCN* expression, metabolic activity, proliferation, morphology and the amount of apoptosis present.

BL1521 inhibited the in situ HDAC activity of a panel of neuroblastoma cell lines by at least 85%. Western analysis showed an increase of histone H3 acetylation in neuroblastoma cells after incubation with BL1521. Northern analysis showed an increase in the expression of $p21^{WAF1/CIP1}$ and a decrease in the expression of *MYCN* in neuroblastoma cells after incubation with BL1521. Proliferation as well as the metabolic activity of neuroblastoma cells decreased significantly in response to treatment with BL1521, regardless of the *MYCN* status of the cells. BL1521 induced poly-(ADP-ribose) polymerase cleavage in a time- and dose-dependent manner, indicating the induction of apoptosis. Furthermore, when compared to the HDAC inhibitors Trichostatin A and 4-phenylbutyrate, BL1521 has an intermediate efficacy. Our results show that BL1521 is a potent inhibitor of HDAC and that HDACs are an attractive target for selective chemotherapy in neuroblastoma.

Keywords: HDAC activity; Trichostatin A; Viability; PARP; Differentiation

1. Introduction

Neuroblastoma is a childhood tumour, which arises from the sympathetic nervous system and has a cumulative incidence of once every 7000 live births [1,2]. Neuroblastoma is the most common solid malignancy in children and is responsible for approximately 15% of all childhood cancer deaths [1–4]. Despite intensive chemotherapeutic regimens the survival of children from metastasized neuroblastoma remains poor and 15–25% of all patients with neuroblastoma will die within 5 years after diagnosis [1,2]. A striking feature of neuroblastoma is its genetic heterogeneity [5]. Some genetic features have been identified to correlate with a clinical outcome. For instance, hyper diploid karyotype and TrkA expression are associated with favorable outcome, leading to spontaneous regression or maturation of the tumour into a benign ganglioneuroma, whereas the amplification of the proto-oncogene *MYCN* and loss of heterozygosity (LOH) of chromosome 1p are associated with a poor prognosis [1,3–7]. The high mortality rate in advanced stage neuroblastoma has inspired the search for new therapeutic agents.

Recently, HDAC have been discovered as a potential target for pharmacological gene therapy in cancer [8–11]. HDACs are abundantly expressed in most tissues and different groups have shown that their function is essential

Abbreviations: HDAC, histone deacetylase; TSA, Trichostatin A; 4PBA, 4-phenylbutyrate; PARP, poly-(ADP-ribose) polymerase; ED_{50}, effective dose were 50% of control value remains

* Corresponding author. Tel.: +31 20 5665958; fax: +31 20 6962596.
E-mail address: a.b.vankuilenburg@amc.uva.nl (A.B.P. van Kuilenburg).

0006-2952/$ – see front matter © 2004 Elsevier Inc. All rights reserved.
doi:10.1016/j.bcp.2004.05.010

for the regulation of gene expression [12,13]. When HDAC function is inhibited, it results in a hyperacetylation of histones. This in turn leads to a looser packaging of DNA around the chromatin, thus facilitating the transcription of genes, resulting in changes in expression of a specific subset of genes (up to 7% of all genes) [12]. These changes in gene expression were shown to lead to a cascade of effects resulting in reduced proliferation and metabolic activity, induction of apoptosis and differentiation of tumour cells in vitro and in vivo [8,14–17].

To date, a number of structurally divers HDAC inhibitors have been identified which differ with respect to their anti-tumour activity, specificity, toxicity and stability [11,12,18]. For example, 4PBA has been extensively studied with many promising results in vitro as well as in vivo [11,17–21]. In one case, it was reported that a patient with leukaemia resistant to treatment achieved complete remission upon treatment with 4PBA [19]. However, due to short half-life of 4PBA a relative high concentration of 4PBA (mM) was needed, hampering the clinical development [22]. Furthermore, butyrate and phenyl butyrate, as compared to for example TSA and Suberoylanilide hydroxamic acid (SAHA), are not specific for HDAC inhibition only as they can also inhibit phosphorylation and methylation of proteins and DNA [23,24]. In addition, the production of the more specific HDAC inhibitor TSA, is a complicated one with a low yield, making it very expensive and this consequently hampers the further application of TSA in a clinical setting [12]. Therefore, the development of novel HDAC inhibitors is warranted. In this study, we have investigated a number of compounds, developed by Beacon Laboratories, which were rationally designed based on the structure of TSA and 4PBA. The resulting compounds were computer tested on their ability to occupy the active site by using the crystal structure of the HDAC enzyme from *Aquifex aeolicus*. This revealed that the compounds were able to extend into the tube like active site in order to be able to displace the Zn^{2+} moiety at the bottom, like TSA does [25]. Our results demonstrate that BL1521, a structural hybrid of 4PBA and TSA, is a potent inhibitor of HDAC activity and has a profound cytotoxic and differentiation-inducing effect in the low micromolar concentration range in neuroblastoma.

2. Materials and methods

2.1. Chemicals and antibodies

BL1521, BL1783, BL1431 and BL1255 were kindly provided to us by Beacon Laboratories Inc. TSA and 4PBA were purchased from Sigma. All compounds were dissolved in DMSO and stored at −20 °C. A mouse monoclonal antibody against PARP was purchased from Biomol. A rabbit polyclonal antibody against acetylated histone H3 was purchased from Upstate Biotech. Both rabbit and mouse secondary antibodies, conjugated to Horseradish peroxidase (HRP), were purchased from DAKO. We purchased ECL-plus and [α-^{32}P]dCTP from Amersham Bioscience. 3-(4,5-Dimethylthiazol-2-yl)-2,5-diphenyltetrazolium bromide (MTT) was purchased from Sigma. Bromo-deoxyuridine (BrdU) proliferation kit, positively charged nylon membrane and complete mini protease inhibitors were purchased from Roche Applied science. The fluorescent HDAC activity kit was purchased from Biomol. SV total RNA isolation system was purchased from Promega. Expresshyb hybridisation mix was purchased from Clontech. QIAquick PCR purification Kit was purchased from Qiagen. Cell culture media, antibiotics and foetal bovine serum were obtained from Invitrogen. All other reagents were of analytical grade.

2.2. Cell culture

The neuroblastoma cell lines were a generous gift from Dr. R. Versteeg (Dept. Human Genetics, Academic Medical Centre, Amsterdam, The Netherlands) and the characteristics have been described in Ref. [26]. The rhabdomyosarcoma cell line (RD), the medulloblastoma cell line (DAOY) and hepatoma cell line (HepG2) were obtained from the American Type Culture Collection. The fibroblast cells we used were control fibroblasts. Cell lines were maintained in medium consisting of RPMI 1640 supplemented with 10% v/v heat inactivated foetal bovine serum, 50 U/ml penicillin/streptomycin, 0.25 μg/ml fungizone, 0.2 mg/ml gentamicin and 4 mM glutamine, at 37 °C in a humidified atmosphere with 5% CO_2. Fibroblast and HepG2 cells were cultured in DMEM under the same conditions and supplements as described above. All incubations of cells with compounds were carried out by preparing a 1:1000 dilution from the DMSO stock solutions in culture medium directly before use.

2.3. Viability

Cells were plated in 96-well plates at a density of 10^4 cells per well and allowed to adhere overnight. The experiments were performed in quadruplicate and started by replacing the medium with fresh medium containing different concentrations of the compounds under investigation. The cells were incubated for various time intervals (24–72 h) with the compounds without refreshing the medium. After the incubation was completed, the metabolic activity was determined using the MTT assay, as described previously [27]. From the dose effect curves ED_{50} values (dose at which 50% of the metabolic activity compared to vehicle control remains) were derived.

2.4. HDAC activity

HDAC activity was measured in situ in neuroblastoma cells using a fluorescent substrate from Fluor-de-lys HDAC

activity kit according to manufacturer's protocol. Briefly; cells were seeded in 96-well plates at a density of 5×10^4 and were allowed to adhere overnight. The following day the medium was replaced by medium containing substrate and BL1521 (0–50 μM) or TSA (1 μM) as a positive control for maximal inhibition. The cells were allowed to deacetylate the substrate for 2 h at 37 °C after which the amount of deacetylated substrate was determined. The substrate can be deacetylated by HDAC1, HDAC2, HDAC3, HDAC4, HDAC8, HDAC9 and SIRT1 enzymes. The amount of fluorescent signal directly reflects the amount of combined HDAC activity that is present.

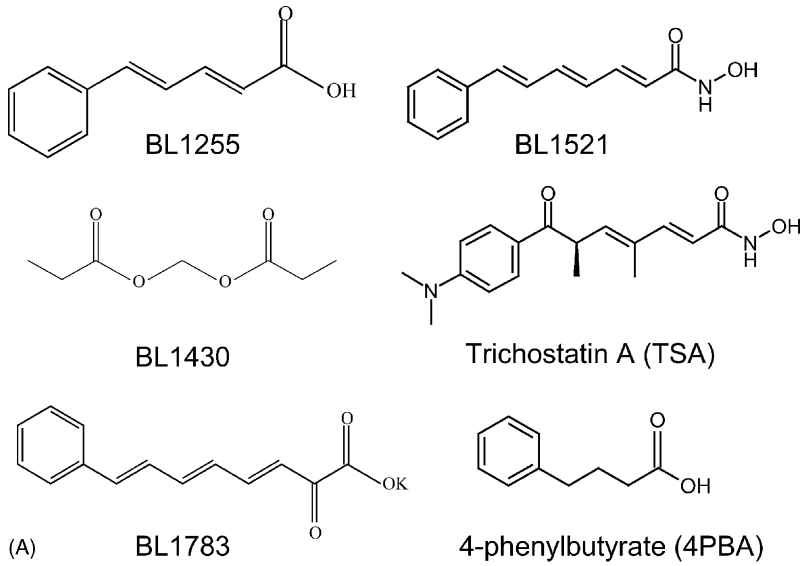

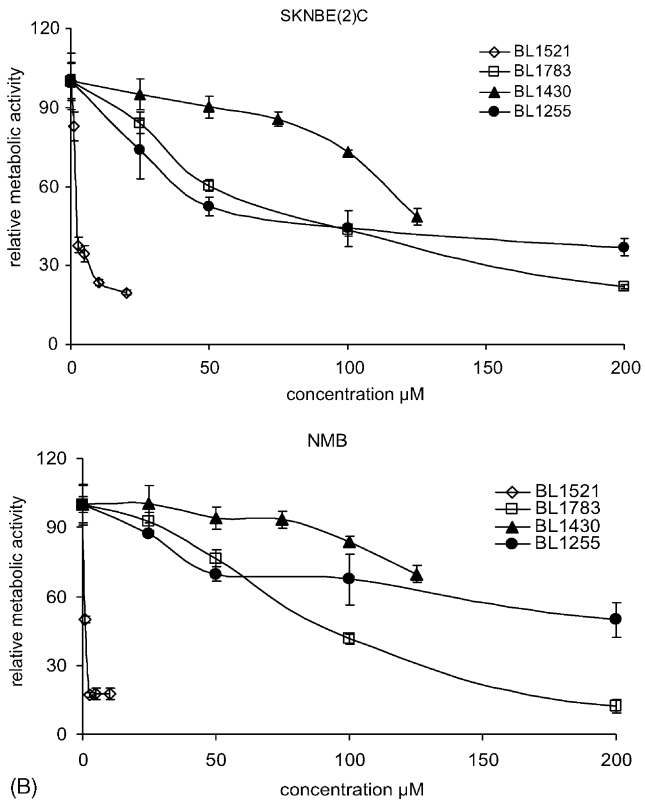

Fig. 1. The effect of Beacon Laboratories compounds on the metabolic activity of the neuroblastoma cell lines SKNBE(2) and NMB. Cells were cultured in the presence of different concentrations of the Beacon Laboratories compounds for 3 days without refreshing the media. Panel A shows the structure of the different compounds we used in our experiments. Panel B shows the reduction of metabolic activity as a result of incubation with Beacon Laboratories compounds in SKNBE(2) and NMB cells as compared to vehicle control treated cells. The experiments are performed in quadruplicate; the values shown are the mean ± S.D.

2.5. Western analysis

For protein analysis cells were grown in 25 cm^2 flasks to 80% confluence. Subsequently, the cells were treated with BL1521 (0–50 μM) or TSA (0–500 nM). The cells were washed with PBS and harvested in medium, counted and collected by centrifugation. The cells were dissolved in ice-cold freshly prepared RIPA buffer (50 mM TrisCl pH 7.5, 150 mM NaCl, 1% NP-40, 0.5% sodium deoxycholate, 0.1% SDS, with protease inhibitors (complete mini, Roche)). Lysates were sonicated and boiled (3 min). Proteins derived from approximately 75×10^4 cells were fractionated on a 10% (w/v) SDS–PAGE mini-gel and transferred to a nitrocellulose membrane. The membrane was blocked with PBS containing 5% (w/v) non-fat milk and 0.01% (v/v) Tween 20 during 1 h at room temperature. Subsequently, the membrane was incubated with primary antibody (anti-PARP at 1:5000 dilution or anti-acetylated H3 at 1 μg/ml) in PBS supplemented with 3% (w/v) non-fat milk and 0.01% (v/v) Tween 20, for 2 h at room temperature. The membrane was washed three times for 5 min with PBS containing 0.01% (v/v) Tween 20 and subsequently incubated with the appropriate secondary antibodies (anti-mouse HRP or anti-rabbit HRP) in PBS containing 3% (w/v) non-fat milk, 0.01% (v/v) Tween 20 for 1 h at room temperature. Subsequently, the membrane was washed three times for 5 min with PBS supplemented with 0.01% (v/v) Tween 20. Detection was performed using chemiluminescence and Bio-Max light film. Equal loading of the gels was determined using ponceau and coomassie staining.

2.6. Northern analysis

For gene expression analysis, cells were grown in 75 cm^2 flasks to 80% confluence. Subsequently, the cells were treated with DMSO, BL1521 (50 μM) or TSA (500 nM) for 16 h. Next, the cells were lysed in SV RNA lysis buffer and RNA was isolated and purified according to the manufacturer's protocol (Promega). For Northern analysis 10 μg (7.4 μg for SKNAS) of total RNA was fractionated on a 1% agarose gel containing 6 M glyoxal (Sigma) and transferred to positively charged nylon membranes (Roche) according to Sambrook et al. [28]. Equal loading of total RNA present in the different lanes on Northern blots was determined using methylene blue. Probes for Northern analysis were amplified by RT–PCR from a neuroblastoma cDNA pool, purified using the QIAquick PCR purification Kit (Qiagen), and radiolabeled using [α-^{32}P]dCTP (Amersham Biosciences) and the random prime labeling system according to Sambrook

Table 1
Anti-tumour efficacy of BL1521, TSA and 4PBA towards a panel of neuroblastoma cell lines

Cell line	4PBA (mM)		BL1521 (μM)		TSA (nM)		Differentiation	AI_{50} (μM)
	MTT	BrdU	MTT	BrdU	MTT	BrdU		
MYCN single								
SKNSH	2.2	3.4	3.0	>10	100	375	++	33
SKNAS*	3.1	4.8	3.7	10	190	>500	−/+	>50
GIMEN*	2.4	4.9	6.0	7.5	420	>500	+	>50
LAN6	3.9	4.3	1.1	9.5	175	495	+	15
SJNB12	4.5	4.5	6.5	15	320	500	−	5
SHEP2	>5	4.5	>10	9.5	500	>500	−	>50
MYCN+								
KCNR	1.2	1.1	12	2.3	80	60	−/+	33
NMB	2.4	1.9	2.2	2.5	180	20	−	33
SKNBE(2)	2.5	3.7	2.3	>10	90	285	−/+	33
SJNB6	4.1	2.5	8.5	>10	90	140	−	>50
AMC106	3.1	4.9	5.1	9.0	>500	>500	−	33
SJNB8*	2.5	4.6	4.5	8.5	270	220	−	>50
N206	2.6	1.9	3.5	7.5	120	70	−	5
SHEP21N*	>5	3.2	>10	>10	>500	220	−	50
SJNB10	>5	4.8	>10	>10	>500	>500	−	>50
Fibroblasts	Nd	Nd	>10	Nd	Nd	Nd	Nd	Nd
HepG2	Nd	Nd	>10	Nd	Nd	Nd	Nd	Nd
RD	4.5	>5	>10	>10	390	500	Nd	Nd
Daoy	4.5	>5	9.2	>10	450	500	Nd	Nd

ED_{50} (columns 1–6) values were determined for metabolic activity and proliferation using MTT and BrdU assays, respectively, after 72 h of treatment. Values shown are the mean of two to six different experiments with each experiment performed in quadruplicate. The cell lines showing induced differentiation, as determined by microscopic inspection, after 4- to 6-day incubation with BL1521 are indicated (also see Fig. 5). ++ indicates extensive outgrowth of neurites from the cells measuring at least twice the length of the cell body and flattening and elongation of the cell body. + indicates outgrowth of neurites from the cells measuring less than two cell body lengths. −/+ indicates a modest increase in neurite length growing from the cells. − indicates no neurite outgrowth was observed. Nd: Not determined. Apoptotic index 50% (AI_{50}) was derived from the PARP western analysis as the concentration at which both fragments of PARP, 113 kDa and 89 kDa, were equally strong after 24 h of treatment with BL1521. *Cell lines sensitive to TRAIL-induced apoptosis. Neuroblastoma cell lines are divided into *MYCN* single copy (*MYCN* single) and *MYCN* amplified (*MYCN*+) subsets.

et al. [28]. $p21^{WAF1/CIP1}$ primers: forward 5′-atgaaattcacccctttcc-3′ and reverse 5′-agcacttcagtgcctccag-3′. *MYCN* primers: forward 5′-cttcggtccagctttctcac-3′ and reverse 5′-tcctgggtaatgagaggtgg-3′. Hybridization was performed at 68 °C using Expresshyb (Clontech) overnight. The blots were washed twice first in 1× SSC, 0.1% w/v SDS at room temperature for 20 min, then in 0.2× SSC, 0.1% w/v SDS at 68 °C for three times 20 min before analysis with the Fuji FLA 3000 phosphor imager.

2.7. Proliferation

Proliferation was measured using a BrdU kit according to manufacturer's protocol. In brief, cells were plated in 96-well plates at a density of 10^4 cells per well and allowed to adhere overnight. The experiments were performed in quadruplicate and started by replacing the medium with fresh medium supplemented with different concentrations of the compounds under investigation. The cells were incubated for 72 h with the compounds without refreshing the medium. Sixteen hours before the end of the experiment, the BrdU labelling solution was added to the wells. The amount of BrdU uptake in the DNA of the cells was subsequently determined by fixation of the cells and incubation with an anti-BrdU-POD antibody followed by colorimetric detection. ED_{50} values were derived from the dose effect curves.

3. Results

The structure of four different compounds: BL1255, BL1430, BL1521 and BL1783 are shown in Fig. 1A. BL1255 is a carboxylic acid with a high resemblance to 4PBA whereas BL1521 contains a hydroxamic acid group like TSA. All compounds contain a phenyl group except

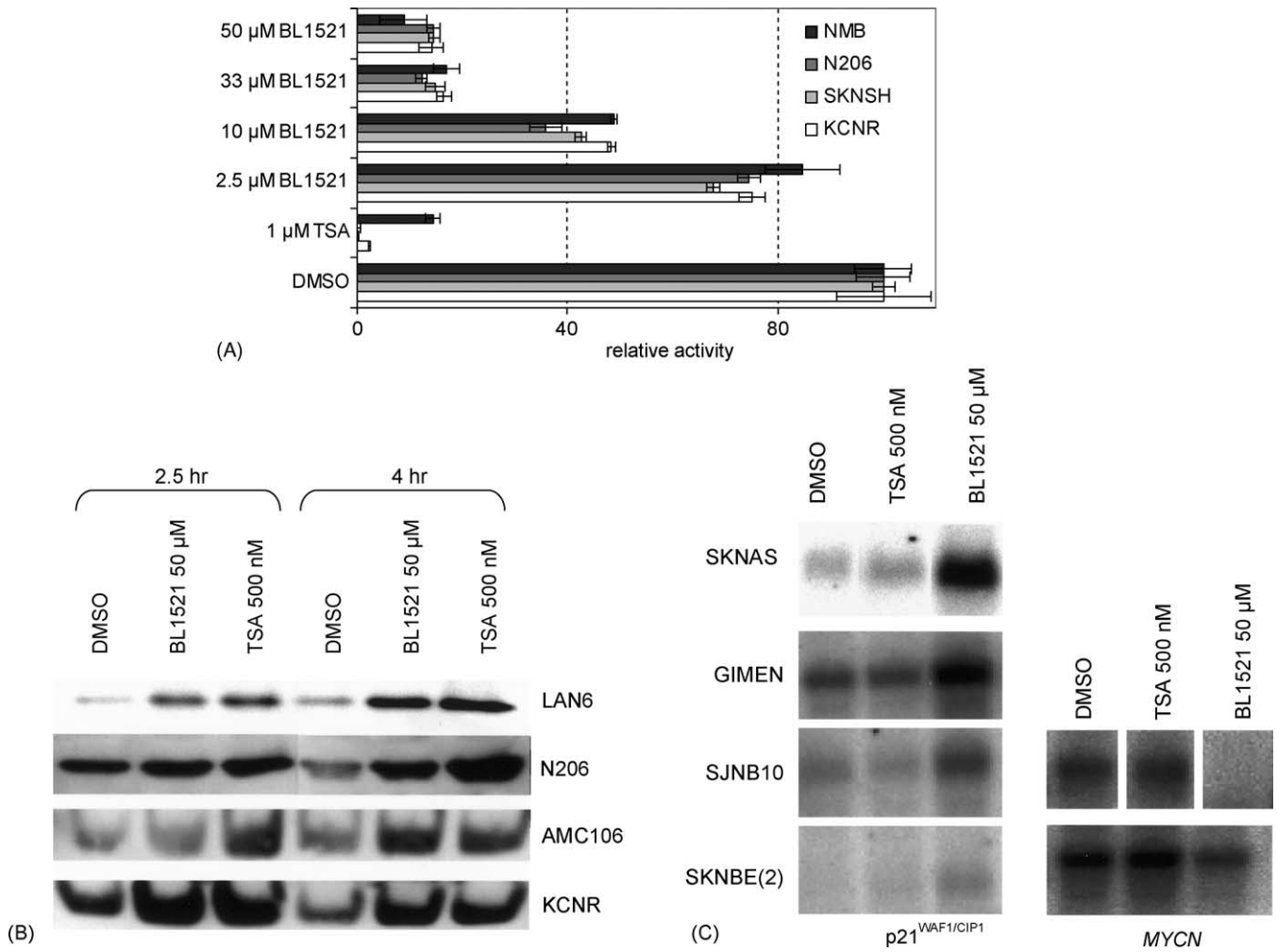

Fig. 2. HDAC inhibitory potential of BL1521. Panel A shows the HDAC activity of different cell lines, at equal cell density, in the presence of positive control TSA (1 µM) or BL1521 (0–50 µM), relative to untreated control. Experiments were performed in triplicate and the bars indicate ±S.D. Panel B shows an immunoblot with the time-dependent increase in histone H3 acetylation as a result of BL1521 (50 µM) or TSA (500 nM) treatment for 2.5 or 4 h of LAN6, N206, AMC106 and KCNR cells. Panel C shows the changes in mRNA expression of $p21^{WAF1/CIP1}$ and *MYCN* as a result of BL1521 (50 µM) or TSA (500 nM) treatment for 16 h of SKNAS, GIMEN, SJNB10 and SKNBE(2) cells.

for BL1430, which is a methylene dipropionate ester. In order to determine the potency of the various compounds, we incubated neuroblastoma cells (SKNBE(2) and NMB) for 72 h with increasing concentrations of the compounds and measured the effect on the metabolic activity using MTT (Fig. 1B). BL1521 is by far the most potent compound in inhibiting the metabolic activity in the two neuroblastoma cell lines (Fig. 1B) with an ED_{50} value of approximately 2.3 μM (Table 1). Both cell lines are least sensitive to BL1430 and have comparable sensitivity BL1783 (carboxylic acid) with an ED_{50} of around 80 μM. SKNBE(2) cells, however, are more sensitive to BL1255 ($ED_{50} = 55$ μM) when compared to NMB cells ($ED_{50} = 220$ μM). The impact of BL1521 on the metabolic activity of fibroblast cells, hepatoma (HepG2), rhabdomyosarcoma (RD) and medulloblastoma (DAOY) is shown in Table 1. On average no significant difference between these cell lines and the neuroblastoma cell lines was found.

The ability of BL1521 to inhibit HDAC activity was measured in situ using a fluorescently labelled HDAC substrate. Fig. 2A shows the relative HDAC activity of four different neuroblastoma cell lines measured in triplicate. TSA at a concentration of 1 μM, almost completely inhibited the HDAC activity in three out of four neuroblastoma cell lines. BL1521 inhibited the HDAC activity in a concentration-dependent manner and at a concentration of 33 μM an inhibition of at least 85% was achieved in all cell lines compared to vehicle treated controls. The average ED_{50} of BL1521 proved to be approximately 8 μM. Western analysis of the amount of acetylated histone H3 revealed an increase after treatment of the neuroblastoma cell lines with BL1521. Representative results are shown in Fig. 2B, showing a clear time-dependent increase of the amount of acetylated histone H3. A moderate to strong induction of $p21^{WAF1/CIP1}$ occurred after treatment with BL1521 (Fig. 2C) in the *MYCN* single copy cell lines SKNAS and GIMEN and the *MYCN* amplified cell lines SJNB10 and SKNBE(2). In contrast, no induction of $p21^{WAF1/CIP1}$ was observed with the HDAC inhibitor TSA. Furthermore, the incubation of the *MYCN* amplified cell lines SJNB10 and SKNBE(2) with BL1521 (50 μM) resulted in a strong reduction of *MYCN* expression, whereas no such effects were observed in the presence of TSA (500 nM) (Fig. 2C).

The time-dependent effect of BL1521 and of the two structurally-related inhibitors, 4PBA and TSA, on the metabolic activity of neuroblastoma cell lines is shown in Fig. 3 and Table 1. At low concentrations all three compounds result in a reduction in metabolic activity compared to the vehicle control. The concentration that is sufficient to reduce the metabolic activity to below starting level ($t = 0$ h) in the neuroblastoma cell line NMB is 2.5 μM, 50 nM and 5 mM for BL1521, TSA and 4PBA, respectively. Table 1 shows that the ED_{50} value on reduction of metabolic activity (MTT) and proliferation (BrdU) after treatment with increasing concentrations of

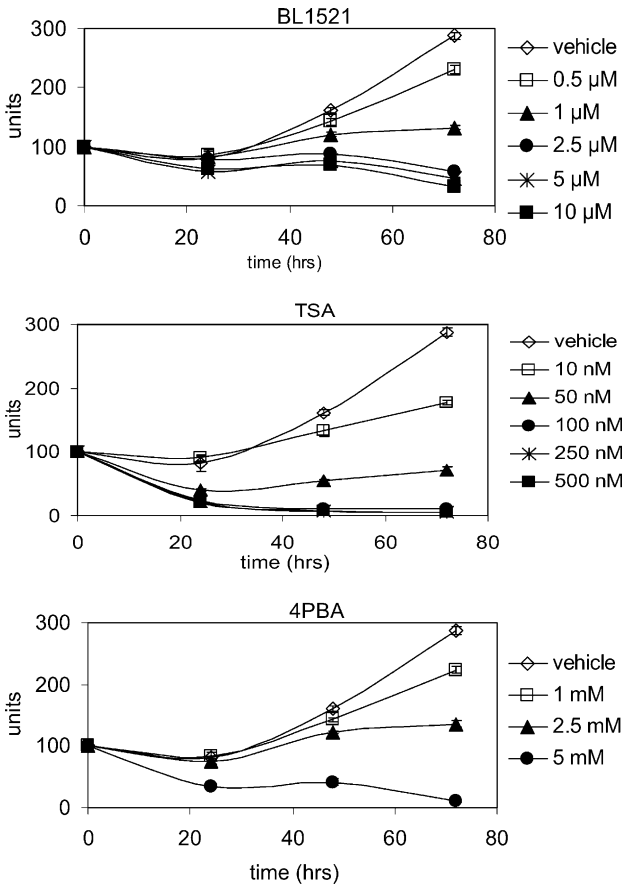

Fig. 3. The effects of BL1521, TSA and 4PBA on the metabolic activity of NMB cells. The cells were cultured for 0–3 days with BL1521 (0–10 μM), TSA (0–500 nM) and 4PBA (0–5 mM). The experiments are performed in quadruplicate; the values shown are the mean ± S.D.

BL1521 for 72 h of a panel of neuroblastoma cell lines is in the low micromolar range for most of the neuroblastoma cell lines (between 1 and 10 μM). It is apparent from this data that both the proliferation and metabolic activity were inhibited in all cell lines by BL1521, TSA and 4PBA. On average, slightly higher ED_{50} values were observed for the inhibition of proliferation (BrdU) when compared to ED_{50} values of the inhibition of metabolic activity (MTT). There appears to be no significant difference in sensitivity towards BL1521 between *MYCN* single copy cell lines and *MYCN* amplified cell lines (Table 1).

Distinct morphological changes of the cells were observed in the presence of BL1521. In order to investigate whether BL1521 is capable of inducing apoptosis, PARP cleavage, a late apoptotic event, was measured. Fig. 4 shows that both BL1521- and TSA-induced apoptosis in neuroblastoma cells in a dose- and time-dependent fashion. Similar results were observed in other neuroblastoma cell lines as well (Table 1). Table 1 shows the 50% apoptotic index (AI_{50}) which was derived from the PARP western analysis as the concentration at which both fragments of PARP were equally strong. This analysis was carried out using protein from cells that were incubated for 24 h with

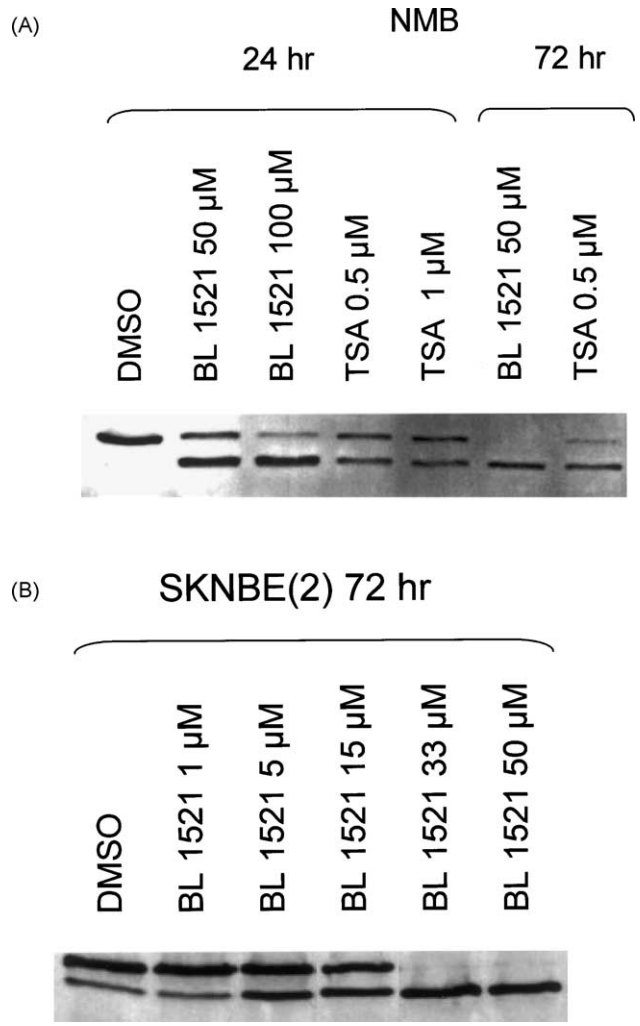

Fig. 4. The time- and dose-dependent induction of PARP cleavage in neuroblastoma cell lines. The cells were cultured for 24–72 h with BL1521 (0–50 μM), TSA (0–1 μM). The molecular weight of full length PARP is 113 kDa, whereas the molecular weight of cleaved PARP is 89 kDa.

increasing concentrations of BL1521. Between the cell lines no obvious correlation between the *MYCN* status and the AI_{50} was found. The four cell lines that are sensitive to TRAIL-induced apoptosis (marked with '∗') are on average slightly less sensitive to BL1521-induced apoptosis, when comparing AI_{50} [29].

Furthermore, we observed a profound induction of differentiation in several cell lines after prolonged treatment with BL1521 at low concentration. Differentiation is characterised by the elongated and more flat shape of the cell body, the increase in neurite length and the amount of neurite connections. Untreated, neuroblastoma cells have a triangular body shape and little or no neurite outgrowth (Fig. 5A, C, E and G). Fig. 5 shows a difference in response to treatment with BL1521 when comparing the morphological changes in *MYCN* single copy (SKNSH and GIMEN) and *MYCN* amplified cell lines (NMB and KCNR). After 4-day incubation with 1 μM BL1521, NMB cells clearly showed no differentiation. SKNSH and GIMEN cells, however, showed extensive differentiation. After 5–6 days incubation with BL1521, the cell bodies were elongated, the neurite length was often more than twice the length of the cell body and there was a high degree of neurite connections. KCNR cells displayed a modest amount of differentiation after 6 days of incubation with BL1521. *MYCN* single copy cell lines proved to be more prone to differentiation upon treatment with BL1521 while the *MYCN* amplified cell lines rarely underwent differentiation (Fig. 5, Table 1).

4. Discussion

This study describes the effects of a newly developed HDAC inhibitor BL1521 on neuroblastoma cells. BL1521 was found to be the most potent one of a number of compounds tested and it is the only compound with a hydroxamic acid group, like TSA, which might explain its effectiveness in inhibiting metabolic activity of neuroblastoma cells.

Neuroblastoma has several characteristic molecular features like loss of heterozygosity, deletion of chromosomes and amplification of genes. Well known is the amplification of *MYCN*, which is a proto-oncogene. *MYCN* amplification occurs in almost 20% of all neuroblastoma tumours and is a prognostic factor for poor survival [1–4]. It has been suggested that the amplification of *MYCN*, which exerts its function through the MYC/MAD/MAX network and Id2 and RB, might be to induce or sustain cell proliferation [24,30,31]. Recently, it has been shown that the HDAC inhibitor MS-275 was able to reduce *MYCN* expression [24]. Our results show that BL1521 is also able to reduce the expression of *MYCN* in *MYCN* amplified cell lines in contrast to TSA, which had no effect on *MYCN* expression. Furthermore, the changes in morphology between the two subsets of neuroblastoma cells show that *MYCN* single copy cell lines are more prone to differentiation than *MYCN* amplified cell lines upon treatment with BL1521. These phenomena, however, did not lead to a significant difference in sensitivity towards BL1521 between *MYCN* single copy cell lines and *MYCN* amplified cell lines, indicating that the mechanism by which HDAC inhibitors affect growth and survival are probably independent of *MYCN*.

To date, the effect of HDAC inhibitors remains illusive, although many research groups have reported that HDAC inhibitors are able to selectively induce the expression of $p21^{WAF1/CIP1}$ [11,17,30,32–34]. Recently, it has been shown that a particular neuroblastoma cell line suffers from difficulties in correctly executing cell cycle arrest due to a dysfunctional $p21^{WAF1/CIP1}$ protein. This resulted in attenuation of G_0–G_1 cell cycle arrest, which might contribute to the genetic aberrations found in this type of tumour [35]. Our results suggest that at least the up-regulation of $p21^{WAF1/CIP1}$ mRNA is still functional in the neuroblastoma cell lines tested since incubation with

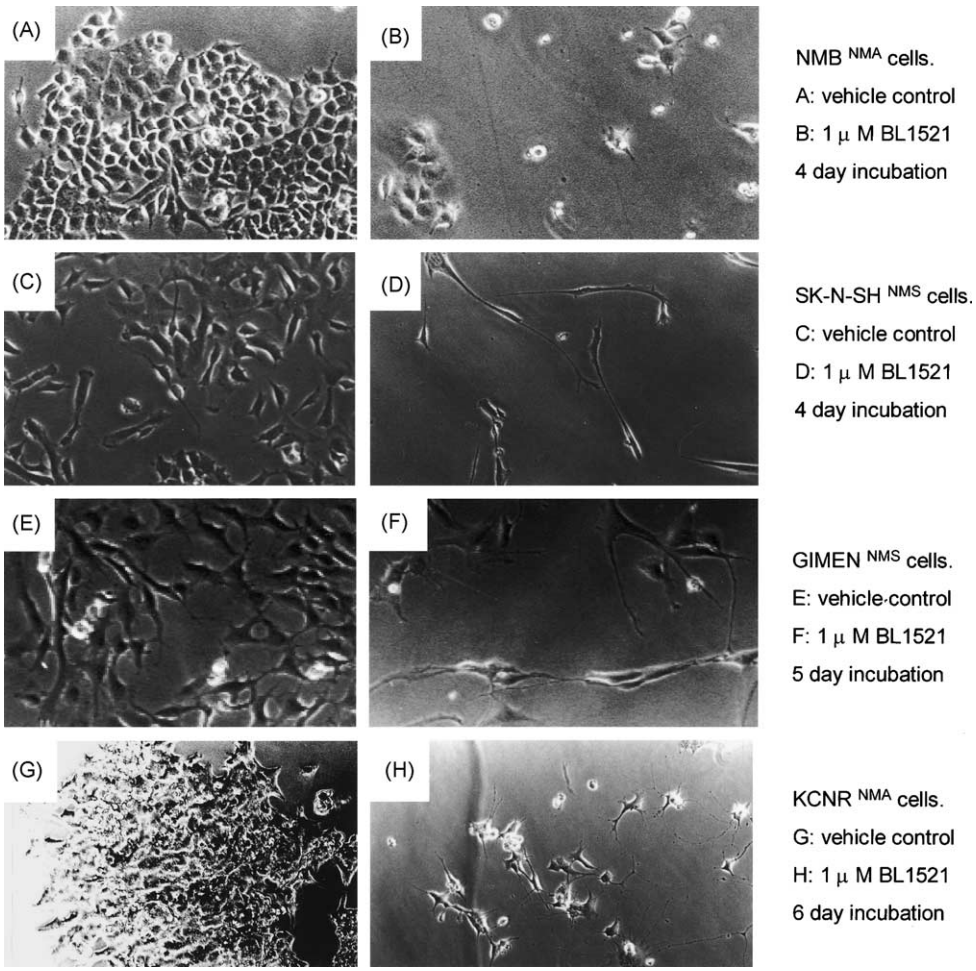

Fig. 5. Different neuroblastoma cell lines showing various amounts of differentiation when treated with BL1521. The panels on the left show vehicle control treated cells. The panels on the right show the cell morphology after treatment for 4–6 days with 1 μM BL1521 without refreshing the medium. Differentiation is characterised by the elongated and more flat shape of the cell body, the increase in neurite length and the amount of neurite connections. NMB cells clearly showed no differentiation after incubation with BL1521. SKNSH and GIMEN cells showed extensive differentiation and KCNR cells display a modest degree of differentiation. NMA, *MYCN* amplified; NMS, *MYCN* single copy.

BL1521 showed an increase of $p21^{WAF1/CIP1}$ mRNA. However, as with *MYCN*, we did not observe an increase of $p21^{WAF1/CIP1}$ mRNA in these neuroblastoma cell lines after incubation with TSA. Thus, although both BL1521 and TSA are believed to inhibit HDACs in a similar fashion due to the hydroxamic acid groups and show a similar response in induction of histone H3 acetylation, we cannot exclude yet any additional effects of BL1521 on the metabolism of the cells besides the inhibition of HDAC.

The neuroblastoma cell lines tested showed a dose- and time-dependent induction of PARP cleavage after incubation with both BL1521 and TSA. PARP cleavage is a late apoptosis event and neuroblastoma is well known for its high prevalence of the absence of caspase 8 expression, resulting in an altered apoptosis pathway [30,36]. Interestingly, we found no significant difference in sensitivity towards the induction of apoptosis after incubation with BL1521 between the TRAIL inducible apoptosis sensitive and insensitive subsets of cell lines. This result might suggest the activation of the mitochondrial apoptosis pathway due to induced cellular stress by BL1521, or, alternatively, the reactivation of caspase 8 signalling via the induced changes in gene expression by BL1521 treatment [29,37,38].

In this study, we showed that BL1521 was capable of reducing the HDAC activity in neuroblastoma cells to 15% or less of control cells. This reduction represents the sum of activity of HDAC1, HDAC2, HDAC3, HDAC4, HDAC8, HDAC9 and SIRT1 due to substrate characteristics. In contrast to classical HDACs, SIRT1 is an HDAC enzyme that needs NADH for its activity. This results in an inability of HDAC inhibitors to effectively inhibit the activity of SIRT1. Our results demonstrate that the SIRT1 activity is very low in most neuroblastoma cell lines since in all of the neuroblastoma cell lines little or no residual HDAC activity could be detected in the presence of TSA. Interestingly, the maximal reduction of HDAC activity achieved in the cell lines tested after incubation with BL1521 is 85% or more. A conceivable explanation for the inability of BL1521 to completely inhibit the HDAC activity might be a difference

in sensitivity of the different HDAC isoforms to inhibition by BL1521. Moreover, it is not yet known which of the classical HDACs are expressed in neuroblastoma cells and to what extend. Analysis of SAGE data suggests that especially HDAC2 might be preferentially expressed in neuroblastoma [12]. BL1521 may prove to be a promising HDAC inhibitor when comparing the effect on neuroblastoma cells to that of TSA and 4PBA. In conclusion, we showed in this study that a new and potent HDAC inhibitor has been developed with promising in vitro results on neuroblastoma cells.

Acknowledgments

We would like to thank Beacon Laboratories Inc. (Phoenix, AZ, USA) for providing us with the compounds. This study was supported by funds granted by the Dutch Cancer Society.

References

[1] Brodeur GM. Neuroblastoma: biological insights into a clinical enigma. Nat Rev Cancer 2003;3:203–16.
[2] Berthold F, Hero B. Neuroblastoma: current drug therapy recommendations as part of the total treatment approach. Drugs 2000;59: 1261–77.
[3] Maris JM, Matthay KK. Molecular biology of neuroblastoma. J Clin Oncol 1999;17:2264–79.
[4] Schwab M. Human neuroblastoma: from basic science to clinical debut of cellular oncogenes. Naturwissenschaften 1999;86: 71–8.
[5] Brodeur GM, Maris JM, Yamashiro DJ, Hogarty MD, White PS. Biology and genetics of human neuroblastomas. J Pediatr Hematol Oncol 1997;19:93–101.
[6] Benard J. Genetic alterations associated with metastatic dissemination and chemoresistance in neuroblastoma. Eur J Cancer 1995;31A: 560–4.
[7] Corvi R, Savelyeva L, Schwab M. Patterns of oncogene activation in human neuroblastoma cells. J Neurooncol 1997;31:25–31.
[8] Marks PA, Richon VM, Rifkind RA. Histone deacetylase inhibitors: inducers of differentiation or apoptosis of transformed cells. J Natl Cancer Inst 2000;92:1210–6.
[9] Jung M. Inhibitors of histone deacetylase as new anticancer agents. Curr Med Chem 2001;8:1505–11.
[10] Kramer OH, Gottlicher M, Heinzel T. Histone deacetylase as a therapeutic target. Trends Endocrinol Metab 2001;12:294–300.
[11] Marks PA, Richon VM, Breslow R, Rifkind RA. Histone deacetylase inhibitors as new cancer drugs. Curr Opin Oncol 2001;13: 477–83.
[12] de Ruijter AJ, van Gennip AH, Caron HN, Kemp S, van Kuilenburg AB. Histone deacetylases (HDACs): characterization of the classical HDAC family. Biochem J 2003;370:737–49.
[13] Dressel U, Renkawitz R, Baniahmad A. Promoter specific sensitivity to inhibition of histone deacetylases: implications for hormonal gene control, cellular differentiation and cancer. Anticancer Res 2000; 20:1017–22.
[14] Butler LM, Zhou X, Xu WS, Scher HI, Rifkind RA, Marks PA, et al. The histone deacetylase inhibitor SAHA arrests cancer cell growth, up-regulates thioredoxin-binding protein-2, and down-regulates thioredoxin. Proc Natl Acad Sci USA 2002;99:11700–5.
[15] Coffey DC, Kutko MC, Glick RD, Butler LM, Heller G, Rifkind RA, et al. The histone deacetylase inhibitor, CBHA, inhibits growth of human neuroblastoma xenografts in vivo, alone and synergistically with all-*trans* retinoic acid. Cancer Res 2001;61:3591–4.
[16] Vigushin DM, Ali S, Pace PE, Mirsaidi N, Ito K, Adcock I, et al. Trichostatin A is a histone deacetylase inhibitor with potent antitumor activity against breast cancer in vivo. Clin Cancer Res 2001; 7:971–6.
[17] Siavoshian S, Segain JP, Kornprobst M, Bonnet C, Cherbut C, Galmiche JP, et al. Butyrate and trichostatin A effects on the proliferation/differentiation of human intestinal epithelial cells: induction of cyclin D3 and p21 expression. Gut 2000;46:507–14.
[18] Kelly WK, O'Connor OA, Marks PA. Histone deacetylase inhibitors: from target to clinical trials. Exp Opin Investig Drugs 2002;11: 1695–713.
[19] Warrell Jr RP, He LZ, Richon V, Calleja E, Pandolfi PP. Therapeutic targeting of transcription in acute promyelocytic leukemia by use of an inhibitor of histone deacetylase. J Natl Cancer Inst 1998;90: 1621–5.
[20] Gore SD, Weng LJ, Zhai S, Figg WD, Donehower RC, Dover GJ, et al. Impact of the putative differentiating agent sodium phenylbutyrate on myelodysplastic syndromes and acute myeloid leukemia. Clin Cancer Res 2001;7:2330–9.
[21] Gilbert J, Baker SD, Bowling MK, Grochow L, Figg WD, Zabelina Y, et al. A phase I dose escalation and bioavailability study of oral sodium phenylbutyrate in patients with refractory solid tumor malignancies. Clin Cancer Res 2001;7:2292–300.
[22] Munster PN, Troso-Sandoval T, Rosen N, Rifkind R, Marks PA, Richon VM. The histone deacetylase inhibitor suberoylanilide hydroxamic acid induces differentiation of human breast cancer cells. Cancer Res 2001;61:8492–7.
[23] Gottlicher M, Minucci S, Zhu P, Kramer OH, Schimpf A, Giavara S, et al. Valproic acid defines a novel class of HDAC inhibitors inducing differentiation of transformed cells. EMBO J 2001;20:6969–78.
[24] Jaboin J, Wild J, Hamidi H, Khanna C, Kim CJ, Robey R, et al. MS-27-275, an inhibitor of histone deacetylase, has marked in vitro and in vivo antitumor activity against pediatric solid tumors. Cancer Res 2002;62:6108–15.
[25] Finnin MS, Donigian JR, Cohen A, Richon VM, Rifkind RA, Marks PA, et al. Structures of a histone deacetylase homologue bound to the TSA and SAHA inhibitors. Nature 1999;401:188–93.
[26] Cheng NC, Chan AJ, Beitsma MM, Speleman F, Westerveld A, Versteeg R. A human modifier of methylation for class I HLA genes (MEMO-1) maps to chromosomal bands 1p35-36.1. Hum Mol Genet 1996;5:309–17.
[27] Carmichael J, DeGraff WG, Gazdar AF, Minna JD, Mitchell JB. Evaluation of a tetrazolium-based semiautomated colorimetric assay: assessment of radiosensitivity. Cancer Res 1987;47:943–6.
[28] Sambrook J, Fritsch EF, Maniatis T. Molecular cloning. 2nd ed. 1989.
[29] van Noesel MM, Pieters R, Voute PA, Versteeg R. The N-myc paradox: N-myc overexpression in neuroblastomas is associated with sensitivity as well as resistance to apoptosis. Cancer Lett 2003;197:165–72.
[30] Borriello A, Roberto R, Della RF, Iolascon A. Proliferate and survive: cell division cycle and apoptosis in human neuroblastoma. Haematologica 2002;87:196–214.
[31] Grandori C, Cowley SM, James LP, Eisenman RN. The Myc/Max/Mad network and the transcriptional control of cell behavior. Annu Rev Cell Dev Biol 2000;16:653–99.
[32] Burgess AJ, Pavey S, Warrener R, Hunter LJ, Piva TJ, Musgrove EA, et al. Up-regulation of p21(WAF1/CIP1) by histone deacetylase inhibitors reduces their cytotoxicity. Mol Pharmacol 2001;60: 828–37.
[33] Richon VM, Sandhoff TW, Rifkind RA, Marks PA. Histone deacetylase inhibitor selectively induces p21WAF1 expression and

gene-associated histone acetylation. Proc Natl Acad Sci USA 2000; 97:10014–9.

[34] Han JW, Ahn SH, Park SH, Wang SY, Bae GU, Seo DW, et al. Apicidin, a histone deacetylase inhibitor, inhibits proliferation of tumor cells via induction of p21WAF1/Cip1 and gelsolin. Cancer Res 2000;60:6068–74.

[35] McKenzie PP, Danks MK, Kriwacki RW, Harris LC. P21Waf1/Cip1 dysfunction in neuroblastoma: a novel mechanism of attenuating G0–G1 cell cycle arrest. Cancer Res 2003;63:3840–4.

[36] Teitz T, Lahti JM, Kidd VJ. Aggressive childhood neuroblastomas do not express caspase-8: an important component of programmed cell death. J Mol Med 2001;79:428–36.

[37] Zimmermann KC, Bonzon C, Green DR. The machinery of programmed cell death. Pharmacol Ther 2001;92:57–70.

[38] Teitz T, Wei T, Valentine MB, Vanin EF, Grenet J, Valentine VA, et al. Caspase 8 is deleted or silenced preferentially in childhood neuroblastomas with amplification of MYCN. Nat Med 2000;6: 529–35.